applied sciences

MDPI

Article

Influence of Medium Composition and Electrode-Relevant Metal Ions on the Amplex Red Fluorescence Readout During High-Voltage Electric Pulse Treatment

Laura Zelencova-Hamarat [1,*], Raminta Rodaitė [1], Rita Saulė [1], Yasin Hamarat [2], Viktorija Skaidrutė Dainauskaitė [1], Kotryna Rastauskaitė [1] and Gintautas Saulis [1,*]

[1] Department of Biology, Vytautas Magnus University, 44404 Kaunas, Lithuania; raminta.rodaite@vdu.lt (R.R.); rita.saule@vdu.lt (R.S.); viktorija.dainauskaite@gmail.com (V.S.D.); kotrynarast@gmail.com (K.R.)
[2] Health Telematics Science Institute, Kaunas University of Technology, 44249 Kaunas, Lithuania; yasin.hamarat@ktu.lt
* Correspondence: laura.zelencova-hamarat@vdu.lt (L.Z.-H.); gintautas.saulis@vdu.lt (G.S.)

Abstract

Amplex Red is a widely used fluorogenic probe for hydrogen peroxide (H_2O_2) detection. In the presence of horseradish peroxidase (HRP), it reacts with H_2O_2 to form fluorescent resorufin. However, during high-voltage electric pulse treatment, fluorescence readouts may be influenced not only by H_2O_2 generation but also by the medium composition, pulse conditions, pH-dependent effects, and metal ions released as a result of electrode corrosion. In this study, we examined how medium composition and selected metal ions relevant to electroporation conditions, such as Fe^{2+}, Fe^{3+}, Al^{3+}, and Cr^{6+}, affect the Amplex Red/HRP/H_2O_2 fluorescence signal. Fluorescence intensity differed markedly among media, with the highest signal in phosphate-buffered saline (PBS, ~34,000 a.u.), followed by HB1 buffer (~19,000 a.u.), cell culture medium (~9000 a.u.), and distilled water (~4100 a.u.). To model ion-mediated interference, metal ions were added directly to the assay mixture. All tested ions reduced fluorescence in a concentration-dependent manner. At 0.4 µM H_2O_2, Fe^{2+} reduced fluorescence by up to 92%, Fe^{3+} by 60%, Al^{3+} by 35%, and Cr^{6+} by 40%. At 10 µM H_2O_2, the quenching effect was reduced but remained evident. In addition, the fluorescence readout showed strong dependence on medium composition and its pH, further demonstrating its vulnerability to the chemical environment. These findings show that the Amplex Red assay is highly sensitive to the assay environment and metal-ion interference. Therefore, it should not be used as a standalone, interference-free measure of H_2O_2 in electroporation-related experiments without appropriate validation controls.

Keywords: Amplex Red; hydrogen peroxide; resorufin; electroporation; fluorescence quenching; electrode corrosion; iron ions; metal-ion interference; assay interference; electric pulse-treated media

Check for updates

Academic Editor: Gang Wei

Received: 26 May 2026
Revised: 11 June 2026
Accepted: 15 June 2026
Published: 5 August 2026

Copyright: © 2026 by the authors. Licensee MDPI, Basel, Switzerland. This article is an open access article distributed under the terms and conditions of the Creative Commons Attribution (CC BY) license.

1. Introduction

Electroporation, also referred to as electropermeabilization, is a widely used technique in cell biology, biotechnology, and medicine for increasing cell membrane permeability by means of short pulses of strong electric field [1,2]. In addition to membrane permeabilization, electric pulse treatment also drives electrochemical reactions at the electrode–solution interfaces [3,4]. These reactions may alter medium composition through pH changes, reactive species formation, and dissolution of electrode material [4–8]. Pronounced spatial pH

changes may occur near the electrodes even when the change in the bulk-medium pH is comparatively limited [6,7].

Stainless-steel electrodes are commonly used in electroporation because of their availability, mechanical stability, and low cost. Previous studies have shown that stainless-steel electrodes are not electrochemically inert under pulsed conditions and may release metal ions into the treated solution [4–7,9–11]. The stainless steel used in the present study belonged to the austenitic 300 series and contained iron, chromium, nickel, manganese, and minor amounts of other metals [12]. Such released ions may precipitate biological macromolecules, alter the chemical properties of the medium, and interfere with analytical readouts [13–15].

Amplex Red (10-acetyl-3,7-dihydroxyphenoxazine) is a widely used fluorogenic probe for H_2O_2 detection. In the presence of horseradish peroxidase (HRP), it reacts with H_2O_2 in a 1:1 stoichiometric manner to form the highly fluorescent product resorufin [16]. Because of its high sensitivity, the assay is frequently used to quantify oxidative activity in biological systems [16–18], including cell electroporation experiments [8,11]. However, the Amplex Red/HRP/H_2O_2 system is not governed exclusively by H_2O_2 concentration. Assay performance depends on the pH, the hydrogen peroxide concentration range, and the surrounding chemical environment, and the signal may also be distorted by reducing substances or other interfering species [19,20].

In the context of electroporation, this raises an important methodological concern. A decrease in Amplex Red fluorescence in pulse-treated samples may reflect a lower apparent signal but not necessarily a lower H_2O_2 concentration. It may also arise from interference caused by medium composition or by metal ions associated with electrode corrosion. Although such effects are plausible, systematic data obtained under electroporation-relevant conditions have remained limited.

The aim of the present study was to examine how pulse-treatment conditions, medium electrical conductivity and composition, selected metal ions relevant to electroporation, and pH-related effects influence the Amplex Red/HRP/H_2O_2 fluorescence readout and to evaluate the implications of these factors for the reliability of hydrogen peroxide detection in pulse-treated systems.

2. Materials and Methods

2.1. Reagents, Media, and Buffer Solutions

Amplex Red reagent (N-acetyl-3,7-dihydroxyphenoxazine, lot 13489098) and horseradish peroxidase (HRP, lot 1138650A) were obtained from Invitrogen/Thermo Fisher Scientific (Waltham, MA, USA). Ferric chloride ($FeCl_3$), ferrous chloride tetrahydrate ($FeCl_2{\cdot}4H_2O$), aluminum chloride hexahydrate ($AlCl_3{\cdot}6H_2O$), potassium dichromate ($K_2Cr_2O_7$), phosphate-buffered saline (PBS, 10× solution, pH 7.2–7.6 at 25 °C, cat. no. P5493-1L), sodium chloride, and other analytical-grade chemicals were purchased from Sigma-Aldrich Chemie (Steinheim, Germany). The 10× PBS contained 1.37 M NaCl, 27 mM KCl, 100 mM Na_2HPO_4, and 18 mM KH_2PO_4. Before use, it was diluted tenfold with ultrapure water to obtain 1× PBS containing 137 mM NaCl, 2.7 mM KCl, 10 mM Na_2HPO_4, and 1.8 mM KH_2PO_4.

HB1 buffer was prepared to contain 136 mM NaCl, 5 mM KCl, 2 mM $MgCl_2$, 2 mM $CaCl_2$, 10 mM HEPES, and 10 mM glucose, adjusted to pH 7.4. Complete cell culture medium consisted of Dulbecco's Modified Eagle's Medium (DMEM, cat. no. D5546, Sigma-Aldrich Chemie, Steinheim, Germany) supplemented with 9% fetal bovine serum, 1% L-glutamine solution, 100 U/mL penicillin, and 100 µg/mL streptomycin. Distilled water was used as a low-ionic-strength and low-conductivity control medium.

A concentrated Amplex Red stock solution was prepared and protected from light. A fresh Amplex Red/HRP working solution was prepared before each experiment by diluting the Amplex Red stock solution in the corresponding assay medium and adding HRP to the same solution. The Amplex Red/HRP working solution added to the microplate wells containing 100 μM Amplex Red and 0.2 U/mL HRP, resulting in final assay concentrations of 50 μM Amplex Red and 0.1 U/mL HRP after mixing with the remaining reaction components. All Amplex Red-containing solutions were protected from light, prepared freshly on the day of each experiment, and maintained at room temperature.

2.2. Electric Pulse Treatment and Electrode Specifications

Electric pulse treatment was performed to simulate electroporation-related conditions. For pulse-exposure experiments, 50 μL aliquots of test medium or Amplex Red/HRP-containing medium were placed between two flat parallel stainless-steel electrodes separated by a 2 mm gap. The electrodes were prepared from stainless-steel plates measuring 50 mm × 10 mm × 1 mm. The stainless steel used for the electrodes consisted mainly of iron, chromium, nickel, manganese, titanium, cobalt, copper, and molybdenum and corresponded to an austenitic 300-series stainless steel [12].

Square-wave electric pulses were applied using a BTX ECM 2001 Electro Cell Manipulator (Harvard Apparatus, Holliston, MA, USA). Depending on the experiment, the pulse duration ranged from 0.1 to 2 ms and the pulse amplitude ranged from 40 to 400 V, corresponding to electric field strengths of 0.2–2.0 kV/cm. Pulse shape and parameters were monitored using a TBS 1072B-EDU oscilloscope (Tektronix U.K. Ltd., Berkshire, UK). After pulse application, treated samples were collected immediately and used for fluorescence measurements.

For direct metal-ion addition experiments, the pulse-treatment step was omitted in order to isolate the effect of selected metal ions on the Amplex Red/HRP/H_2O_2 fluorescence readout independently of pulse-induced electrochemical reactions.

2.3. Amplex Red Fluorescence Assays

Fluorescence assays were performed to evaluate the influence of medium composition, electric pulse exposure, pulse parameters, pH conditions, and electrode-relevant metal ions on the Amplex Red/HRP fluorescence readout. Reactions were performed in black 96-well plates using freshly prepared Amplex Red/HRP working solution, and fluorescence intensity was measured immediately at room temperature using a spectrofluorimeter Genios Pro (Tecan Austria GmbH, Salzburg, Austria). Excitation and emission wavelengths were 535 nm and 590 nm, respectively. Experiments were performed on three separate days using freshly prepared media and reagents.

To evaluate the effect of medium composition on the Amplex Red/HRP/H_2O_2 assay, reaction mixtures were prepared in PBS, HB1 buffer, complete DMEM, or distilled water. Each well contained 10 μL of H_2O_2 solution, 40 μL of the respective medium, and 50 μL of Amplex Red/HRP working solution, giving a final volume of 100 μL. The final assay concentrations were 0.4 μM H_2O_2, 50 μM Amplex Red, and 0.1 U/mL HRP.

To evaluate fluorescence formation after electric pulse treatment in different media, Amplex Red/HRP-containing solutions were prepared in PBS, HB1 buffer, complete DMEM, or distilled water. For each condition, 50 μL of the corresponding Amplex Red/HRP-containing medium was placed between stainless-steel electrodes and exposed to 1 or 3 rectangular electric pulses of 100 V amplitude and 2 ms duration. Non-pulsed samples served as controls. Immediately after treatment, samples were transferred to a 96-well plate, and fluorescence intensity was measured.

To examine the effect of pulse parameters on the Amplex Red fluorescence readout, Amplex Red/HRP-containing medium was exposed to single rectangular electric pulses of different amplitudes and durations. Pulse amplitudes of 100–400 V and pulse durations of 0.5 and 2 ms were applied, and fluorescence was measured immediately after pulse treatment. This experiment was used to determine whether an increasing electrical load produced a monotonic increase in fluorescence or whether signal suppression occurred under stronger pulse conditions.

The effect of pH on the Amplex Red/HRP/H_2O_2 fluorescence response was assessed using pH-adjusted citrate, phosphate, borate, and glycine buffer systems. H_2O_2 dilutions were prepared in the corresponding pH-adjusted buffers and mixed with Amplex Red/HRP working solution in a 1:1 ratio in 96-well plates. The final H_2O_2 concentrations ranged from 0.02 to 2 µM. This experiment was performed to determine whether pH-dependent changes in the assay environment affected resorufin fluorescence formation.

For metal-ion interference experiments, Fe^{2+}, Fe^{3+}, Al^{3+}, and Cr^{6+} solutions were added directly to the Amplex Red/HRP/H_2O_2 reaction mixture. Ferric chloride and ferrous chloride tetrahydrate were dissolved separately in distilled water to prepare Fe^{3+} and Fe^{2+} stock solutions, respectively. Aluminum chloride hexahydrate and potassium dichromate were dissolved in 0.9% NaCl to prepare Al^{3+} and Cr^{6+} stock solutions. Working solutions were then prepared freshly from these stocks to obtain the required final concentrations.

For each metal-ion assay, the wells contained 10 µL of metal-ion solution, 10 µL of H_2O_2 solution, 30 µL of PBS or the corresponding assay medium, and 50 µL of Amplex Red/HRP working solution, giving a final reaction volume of 100 µL. Control wells contained the corresponding vehicle solution instead of metal ions. Two final H_2O_2 concentrations were tested: 0.4 µM and 10 µM. The 10 µM H_2O_2 concentration was selected as a higher peroxide-availability condition to evaluate whether metal-ion-mediated fluorescence suppression persists when the assay is less limited by H_2O_2 availability. The tested final concentration ranges were 0.01–5.0 mM for Fe^{2+}, Fe^{3+}, and Al^{3+}, and 0.1–1000 µM for Cr^{6+}.

2.4. Electrical Conductivity Measurement of Media

The electrical conductivity of the tested media was determined by conductometric analysis. Measurements were performed for distilled water, HB1 buffer, PBS, and cell culture medium using platinum electrodes. Because the exact electrode surface area and distance between electrodes were not known, the cell constant was determined using a 100 mM KCl standard solution. The resistance of the KCl standard and each tested medium was measured using an LCR E7-11 conductometer, and the specific electrical conductivity was calculated from the measured resistance and the determined cell constant. Conductivity values were expressed as S/m.

2.5. Determination of Nickel and Chromium Release from Stainless-Steel Electrodes

To evaluate the release of nickel and chromium ions from stainless-steel electrodes during pulse exposure, filtered sterile 0.9% NaCl solution was placed in a stainless-steel cuvette and exposed to rectangular electric pulses of 2 ms duration. The electric field strength was varied from 0.2 to 1.2 kV/cm. After pulse treatment, the solution was collected from the cuvette, and nickel and chromium ion concentrations were determined by atomic absorption spectrophotometry using a Perkin Elmer (Waltham, MA, USA) Zeeman 30/30 instrument. These measurements were performed to assess whether pulse-treated media could contain electrode-derived contaminants at concentrations relevant to analytical interference.

2.6. Data Presentation and Analysis

Data are presented as averages of three independent experiments (n = 3), each performed on a separate day with freshly prepared media and reagents. Fluorescence values were expressed either as absolute fluorescence intensity or as values normalized to the corresponding control condition, as indicated in the figure legends. For medium-comparison analyses, PBS was used as the reference condition and set to 100%. For metal-ion experiments, fluorescence intensity was expressed relative to control wells without added metal ions. Raw data were organized in Microsoft Excel (Microsoft Corporation, Redmond, WA, USA), and graphs were prepared using SigmaPlot 11.0 (Systat Software Inc., San Jose, CA, USA).

3. Results

3.1. Dependence of Fluorescence Response of the Amplex Red/HRP System on Electric Treatment Parameters in Different Media

Recently, the formation of reactive oxygen species including hydrogen peroxide in the medium treated with high-voltage pulses has been demonstrated [8,21]. However, more detailed analysis on the dependence of ROS generation on the various parameters of electric treatment is needed. Here, the formation of hydrogen peroxide in various media as a result of the treatment with high-voltage electric pulses has been studied under various exposure conditions. The formation of H_2O_2 was evaluated based on the fluorescence of Amplex Red/HRP System [8,16].

When Amplex Red/HRP-containing media were exposed to rectangular electric pulses with an amplitude of 100 V (electric field strength of 0.5 kV/cm) and a duration of 2 ms, fluorescence intensity increased with increasing pulse number (Figure 1a). After one pulse, the fluorescence signal was highest in PBS, followed by complete DMEM and HB1 buffer, while distilled water remained close to background. After three pulses, PBS again showed the highest fluorescence intensity, reaching approximately 4500 a.u., whereas complete DMEM reached approximately 2000 a.u., HB1 approximately 1100–1200 a.u., and distilled water remained very low, approximately 100 a.u.

Then the influence of pulse amplitude and pulse duration on Amplex Red fluorescence was evaluated in distilled water. After the application of a single short pulse of 0.5 ms duration, the fluorescence intensity increased with increasing pulse voltage (Figure 1b). Under these conditions, the fluorescence response followed the expected monotonic order, with higher voltage producing higher fluorescence intensity.

However, this monotonic relationship was not preserved when pulse duration was increased to 2 ms (Figure 1b). Under the longer pulse condition, the fluorescence signal measured after a 200 V pulse was lower than that measured after a 100 V pulse. Thus, increasing the electrical load did not always produce a higher fluorescence response. This non-monotonic behavior shows that fluorescence intensity did not increase proportionally with electrical load under these conditions.

3.2. Relationship Between Medium Electrical Conductivity and Pulse-Induced Fluorescence

The intensity of electrochemical reactions during electric pulse treatment depends strongly on electric current density, which is determined by the electrical conductivity of the medium. Therefore, it can be expected that the intensity of the hydrogen peroxide formation would depend on the specific conductance of each medium. To ascertain whether this assumption is correct, the electrical conductivities of the tested media were determined and compared with their corresponding pulse-induced fluorescence responses.

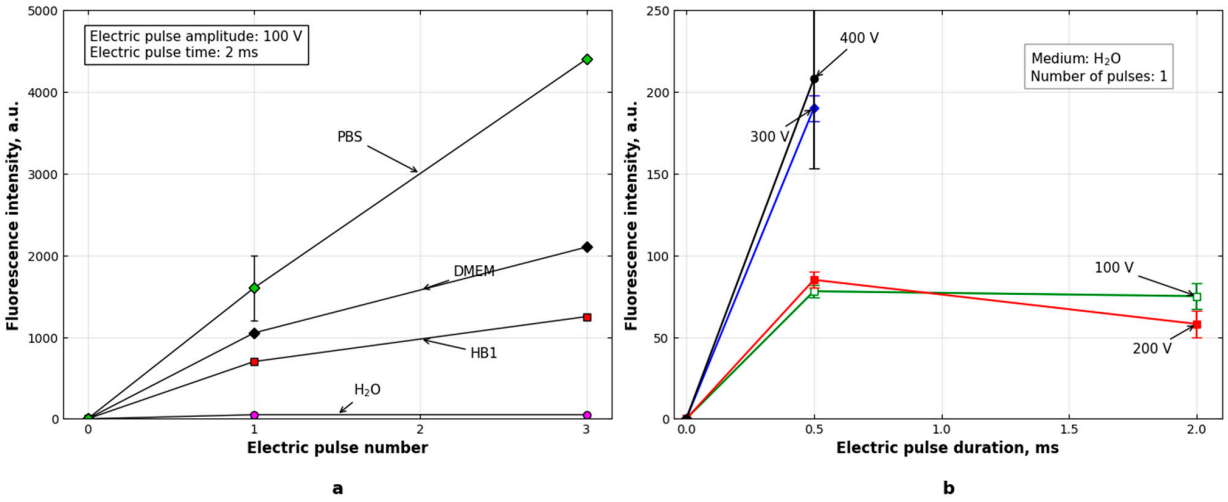

Figure 1. Dependence of Amplex Red fluorescence intensity on electric treatment parameters in different media. (**a**) Fluorescence intensity measured in PBS, HB1 buffer, complete DMEM, and distilled water after exposure to 0 to 3 rectangular electric pulses. Markers indicate the different media: green diamonds (PBS), black diamonds (DMEM), red squares (HB1), and magenta circles (H_2O_2). Pulse parameters were an amplitude of 100 V and a duration of 2 ms. (**b**) Dependence of Amplex Red fluorescence intensity on pulse duration and pulse amplitude in distilled water. Fluorescence was measured after application of single rectangular electric pulses at different voltages and pulse durations. The figure illustrates the appearance of non-monotonic signal behavior under higher electrical load. Media contained Amplex Red and horseradish peroxidase during pulse treatment. Values are presented as means ± SD of three independent experiments (n = 3).

PBS and HB1 buffer showed the highest conductivities: 0.865 S/m and 0.678 S/m, respectively. The conductivity of complete DMEM was considerably lower, 0.169 S/m, whereas distilled water showed the lowest conductivity, 2.52×10^{-3} S/m. To allow direct comparison between conductivity and fluorescence responses, conductivity values for all media were normalized to the one of PBS, which was set as 100% (Figure 2a). The normalized electrical conductivities of HB1, complete DMEM, and distilled water were 78.4%, 19.5%, and 0.3% of the PBS value, respectively (Figure 2a).

For the direct comparison of pulse-induced fluorescence (Figure 1a) with electrical conductivities of media (Figure 2a), the responses of Amplex Red/HRP/H_2O_2 system in each medium were normalized to the corresponding PBS fluorescence value obtained under the same pulse conditions. Thus, the two bars shown for HB1 buffer, complete DMEM, and distilled water in Figure 2b represent the relative fluorescence intensities after one and three pulses, respectively.

Comparison of Figure 1a,b showed that the conductivity pattern followed the pulse-induced fluorescence trend, with PBS and HB1 being more conductive than complete DMEM and distilled water. After one pulse, HB1, complete DMEM, and distilled water retained approximately 41.2%, 64.7%, and 3.7% of the PBS fluorescence signal, respectively (Figure 2b). After three pulses, the corresponding values were approximately 25.8%, 44.6%, and 2.5% (Figure 2b).

However, the correspondence was incomplete. HB1 had a conductivity relatively close to PBS but produced markedly lower fluorescence. In addition, the fluorescence differences between media were more pronounced than would be expected from conductivity alone. These results indicate that: (i) both the standard H_2O_2 calibration response and the pulse-induced fluorescence response are strongly medium dependent and (ii) despite that electrical conductivity of the medium is one of the main factors determining the intensity

of the pulse-induced fluorescence of Amplex Red/HRP/H_2O_2 system, it does not fully explain the medium-dependent differences in the Amplex Red readout.

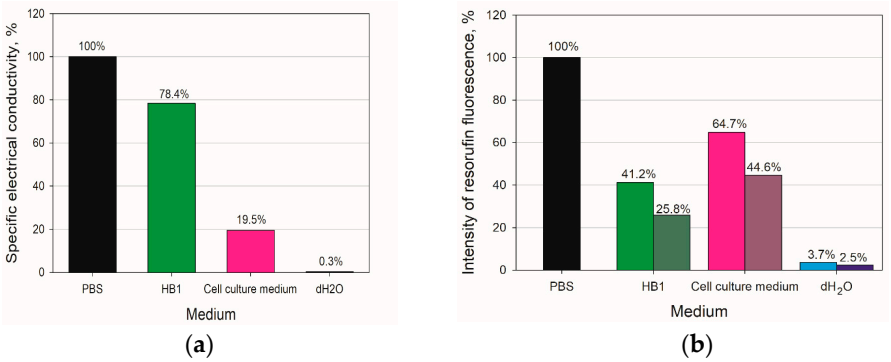

(**a**) (**b**)

Figure 2. Comparison between relative medium electrical conductivity and relative resorufin fluorescence intensity. (**a**) Electrical conductivities of the tested media normalized to PBS. (**b**) Resorufin fluorescence intensities normalized to the corresponding PBS value. In panel (**b**), the two bars for HB1, cell culture medium, and distilled water represent the relative fluorescence after one and three rectangular electric pulses, respectively. Pulse parameters were 100 V amplitude and 2 ms duration. The figure illustrates that conductivity alone does not fully account for the fluorescence response observed in different media.

3.3. Medium-Dependent Fluorescence Response of the Amplex Red/HRP/H_2O_2 System

To check whether the fluorescence response of the Amplex Red/HRP/H_2O_2 system depends on the medium used, it was evaluated in PBS, HB1 buffer, complete DMEM, and distilled water using exogenously added H_2O_2. As shown in Figure 3, fluorescence intensity increased with increasing H_2O_2 concentration in all tested media. However, the absolute fluorescence response differed markedly among media despite identical nominal H_2O_2 concentrations.

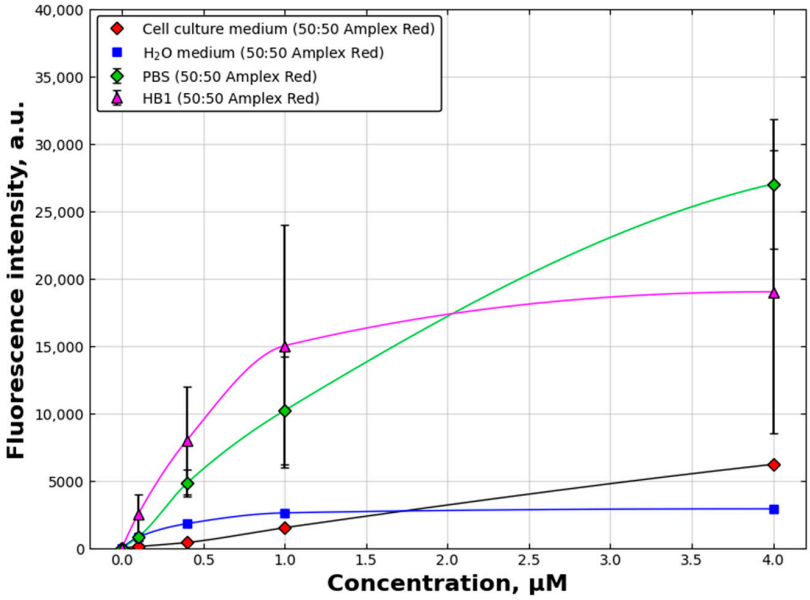

Figure 3. Fluorescence response of the Amplex Red/HRP/H_2O_2 system in PBS, HB1 buffer, complete DMEM, and distilled water as a function of H_2O_2 concentration. Reaction mixtures contained Amplex Red, horseradish peroxidase, and the indicated concentrations of H_2O_2.

At the highest tested H_2O_2 concentration, PBS produced the strongest fluorescence signal, reaching approximately 34,000 a.u. HB1 buffer produced a lower but still substantial response of approximately 19,000 a.u., whereas complete DMEM reached approximately

9000 a.u. Distilled water produced the weakest response, approximately 4100 a.u. Thus, when normalized to the PBS signal, HB1 retained approximately 55.8% of the PBS response, while complete DMEM and distilled water retained only 26.3% and 12.0%, respectively. These results demonstrate that the same nominal H_2O_2 concentration does not generate the same Amplex Red fluorescence output in different media.

3.4. Nickel and Chromium Release from Stainless-Steel Electrodes During Pulse Exposure

When stainless-steel electrodes are used, ferric and/or ferrous, chromium, nickel, and manganese ions are released from the anode into the solution and concentrations of iron ions have been determined in a number of cell electroporation experiments [5,6,9,12,13]. Meanwhile, concentrations of other ions are rarely determined.

To evaluate whether pulse-treated media in our experiments may also contain nickel and chromium ions released from stainless-steel electrodes, their concentrations were determined after pulse exposure. Filtered sterile 0.9% NaCl solution was exposed to a rectangular electric pulse of 2 ms duration at voltages ranging from 40 V to 240 V corresponding to electric field strengths ranging from 0.2 to 1.2 kV/cm. After pulse treatment, metal-ion concentrations were determined by atomic absorption spectrophotometry. Nickel and chromium were selected because they are characteristic alloying elements of austenitic stainless steel and therefore serve as specific indicators of electrode dissolution during pulse exposure.

Both nickel and chromium ions were detected in the medium after pulse exposure, and their concentrations increased with increasing electric field strength (Figure 4). At 0.8 kV/cm and 2 ms, nickel ion concentration reached approximately 0.05 mM, whereas chromium ion concentration reached approximately 0.04 mM. These results confirm that besides iron ions stainless-steel electrodes can also release nickel an chromium ions into the surrounding medium during electric pulse treatment.

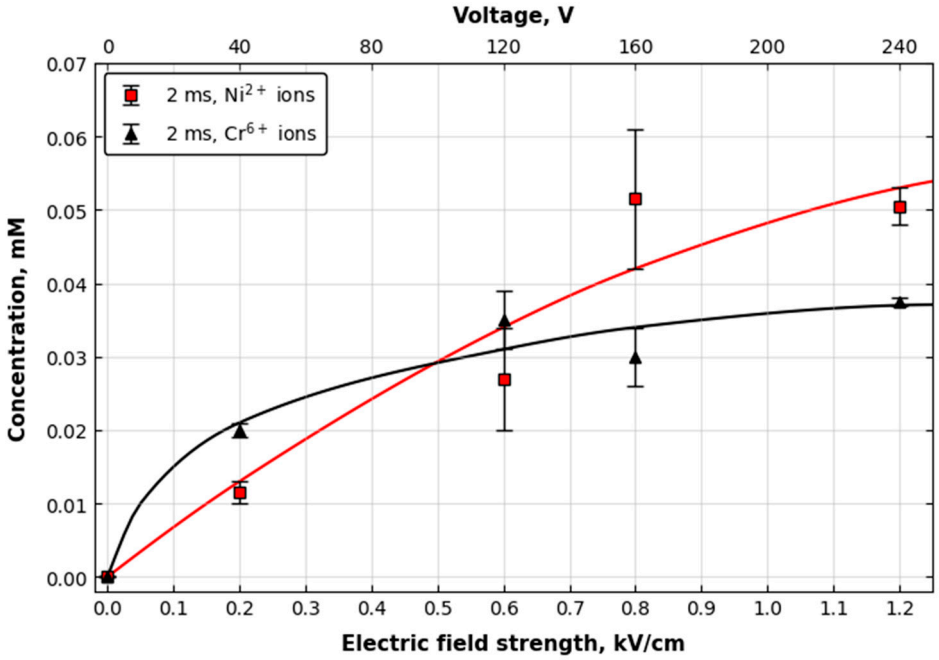

Figure 4. Concentrations of nickel and chromium ions released from stainless steel electrodes into the electroporation medium as a function of electric field strength during a 2 ms rectangular pulse. Metal-ion concentrations were determined by atomic absorption spectrophotometry in 0.9% NaCl after pulse exposure.

3.5. Metal-Ion-Mediated Fluorescence Suppression at Low H_2O_2 Concentration

The direct effects of electrode-relevant metal ions on the Amplex Red/HRP/H_2O_2 fluorescence readout were first evaluated at the low H_2O_2 concentration of 0.4 µM. Under these conditions, all tested ions reduced the fluorescence signal, although the magnitude of suppression differed substantially among ions. Al^{3+} was included because the electrodes made of aluminum alloy are used in many comercially available electroporation cuvettes [22], while it is known that aluminum ions can be released from both the anode and the cathode as a result of the exposure of cuvettes to high-voltage pulses [4,6,14]. This makes Al^{3+} relevant to the evaluation of electrode-associated fluorescence interference.

Fe^{2+} produced the strongest concentration-dependent reduction in fluorescence. The signal decreased by approximately 45% at 0.1 mM Fe^{2+}, by approximately 78% at 1 mM Fe^{2+}, and by up to 92% at 5 mM Fe^{2+} compared with control wells without added metal ions (Figure 5a). Fe^{3+} also reduced fluorescence, although less strongly than Fe^{2+}, producing approximately 20% reduction at 0.1 mM and up to 60% reduction at the highest tested concentration (Figure 5b).

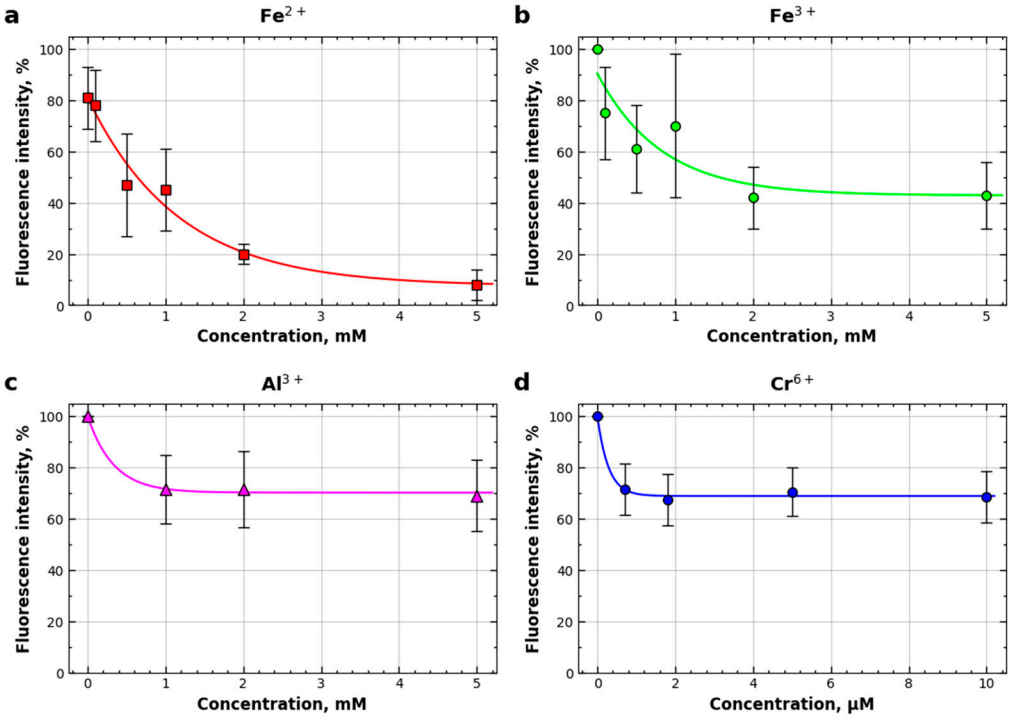

Figure 5. Concentration-dependent effects of Fe^{2+}, Fe^{3+}, Al^{3+}, and Cr^{6+} on Amplex Red fluorescence at low H_2O_2 concentration. Fluorescence intensity is expressed as a percentage of the corresponding control without added metal ions. The final H_2O_2 concentration was 0.4 µM. Values are presented as means ± SD of three independent experiments (n = 3). (**a**) Fe^{2+}; (**b**) Fe^{3+}; (**c**) Al^{3+}; (**d**) Cr^{6+}.

Al^{3+} and Cr^{6+} produced weaker but still evident suppressive effects on fluorescence. Al^{3+} reduced fluorescence by approximately 35% at the highest concentration shown (Figure 5c), whereas Cr^{6+} reduced fluorescence by approximately 40% (Figure 5d). Thus, at low H_2O_2 concentration, the apparent strength of fluorescence suppression followed the order $Fe^{2+} > Fe^{3+} > Cr^{6+} \approx Al^{3+}$. These results show that several electrode-relevant metal ions can distort the Amplex Red fluorescence readout, with iron ions producing the strongest effect.

3.6. Metal-Ion-Mediated Fluorescence Suppression at High H_2O_2 Concentration

To determine whether metal-ion interference depends on peroxide availability, the experiments were repeated at a higher H_2O_2 concentration of 10 µM. Under these conditions, the relative fluorescence reduction caused by all tested ions was smaller than that observed at 0.4 µM H_2O_2.

Fe^{2+} remained the strongest suppressor, but its maximum effect was reduced to approximately 25% fluorescence reduction (Figure 6). Fe^{3+}, Al^{3+}, and Cr^{6+} produced weaker effects at 10 µM H_2O_2, generally remaining within approximately 10–20% fluorescence reduction at the highest tested concentrations (Figure 6). Thus, increasing H_2O_2 concentration reduced the relative impact of metal-ion-mediated signal suppression.

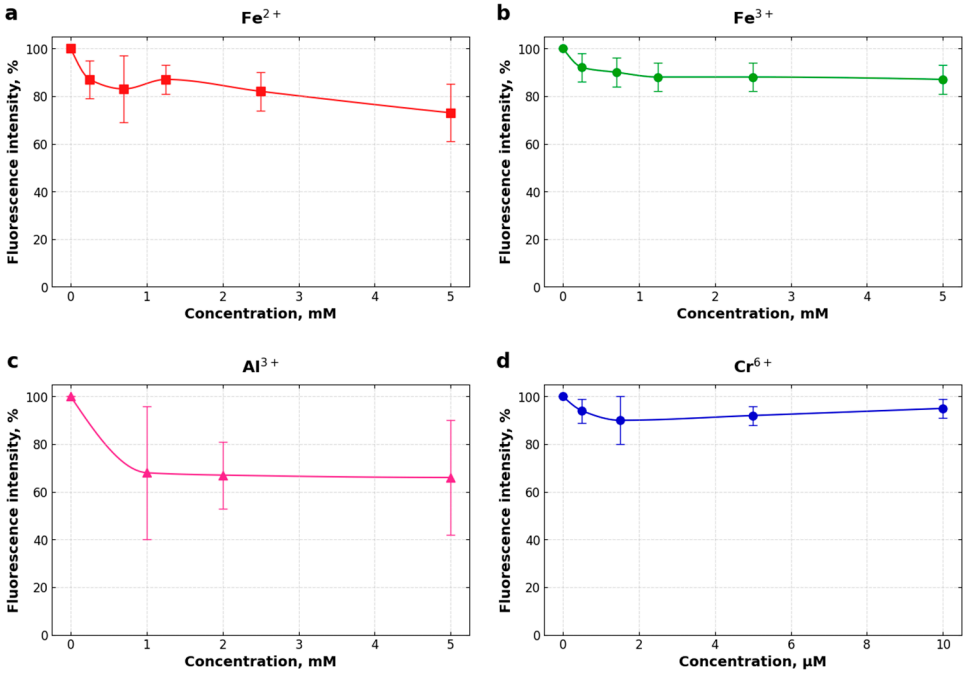

Figure 6. Concentration-dependent effects of Fe^{2+}, Fe^{3+}, Al^{3+}, and Cr^{6+} on Amplex Red fluorescence at high H_2O_2 concentration. Fluorescence intensity is expressed as a percentage of the corresponding control without added metal ions. The final H_2O_2 concentration was 10 µM. Values are presented as means ± SD of three independent experiments (n = 3). (**a**) Fe^{2+}; (**b**) Fe^{3+}; (**c**) Al^{3+}; (**d**) Cr^{6+}.

These results indicate that ion-mediated interference is most pronounced under low-peroxide conditions. When H_2O_2 was more abundant, HRP-catalyzed resorufin formation appeared to become less vulnerable to competing suppressive processes, although interference remained detectable.

3.7. Comparison of Maximum Fluorescence Reduction at Low and High H_2O_2 Concentrations

To summarize the concentration-dependent ion effects, the maximum observed fluorescence reductions caused by each ion were compared at 0.4 µM and 10 µM H_2O_2. At 0.4 µM H_2O_2, the maximum reductions were approximately 92% for Fe^{2+}, 60% for Fe^{3+}, 40% for Cr^{6+}, and 35% for Al^{3+}. At 10 µM H_2O_2, the maximum reductions were lower for all ions, with Fe^{2+} causing approximately 25% reduction and Fe^{3+}, Al^{3+}, and Cr^{6+} remaining within the range of approximately 10–20% (Figure 7).

This comparison confirms that the Amplex Red fluorescence readout is especially vulnerable to metal-ion-mediated suppression when peroxide concentration is low. Therefore, ion interference may be particularly important in electroporation-related experiments where H_2O_2 formation is expected to be modest or localized.

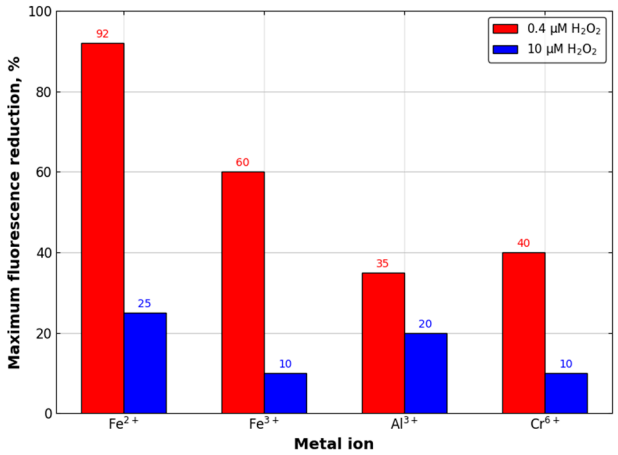

Figure 7. Maximum observed reduction in Amplex Red fluorescence caused by selected metal ions at two H_2O_2 concentrations. Bars show the highest reduction in fluorescence observed for Fe^{2+}, Fe^{3+}, Al^{3+}, and Cr^{6+} at 0.4 μM and 10 μM H_2O_2 under the tested conditions.

3.8. Effect of pH and Buffer System on the Amplex Red Readout

The effect of pH and buffer system on the Amplex Red fluorescence response was evaluated using pH-adjusted citrate (pH 2–5), phosphate (pH 5–8), and borate (pH 8–9), buffer systems. Fluorescence intensity changed substantially across the tested pH range and depended on both pH and H_2O_2 concentration (Figure 8). The strongest fluorescence responses were observed under near-neutral to mildly alkaline conditions, whereas more acidic conditions produced lower fluorescence (Figure 8). The response also varied with H_2O_2 concentration, indicating that both hydrogen peroxide availability and pH-dependent assay chemistry contributed to the final fluorescence output.

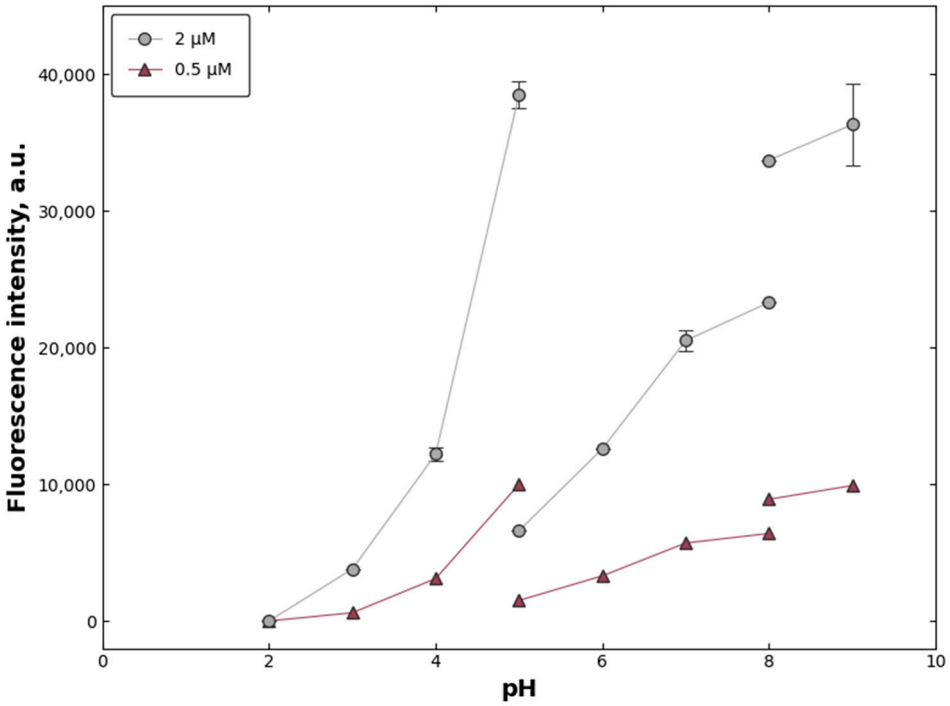

Figure 8. Effect of pH on the fluorescence readout of the Amplex Red assay. Fluorescence measurements were performed at different pH values using citrate (pH 2–5), phosphate (pH 5–8), and borate (pH 8–9) buffer systems and H_2O_2 concentrations of 0.5 and 2 μM. Values represent averages of three independent experiments.

Moreover, large differences between fluorescence even at the same pH and H_2O_2 concentrations were observed when different buffer systems were used. For example, at H_2O_2 concentration equal to 2 μM, the fluorescence of Amplex Red/HRP/H_2O_2 system reached about 38,650 a.u. in citrate buffer with pH 5.0, while it was only about 6720 in phosphate buffer with the same pH value (Figure 8). The differences between tthe fluorescence in phospate and borate buffer systems were not so huge but still substantial. For example, at H_2O_2 concentration equal to 2 μM, the fluorescence was about 38,650 a.u. in citrate buffer with pH 5.0, while it was only about 6720 in borate buffer respectively (Figure 8).

These results demonstrate that the fluorescence signal of Amplex Red/HRP/H_2O_2 system is not determined by H_2O_2 concentration alone. The pH of solution and and buffer composition are additional factors that can influence the Amplex Red/HRP/H_2O_2 fluorescence readout.

4. Discussion

The present study examined how electric pulse parameters, electrical conductivity, medium composition, pH conditions, and as well as electrode-relevant metal ions influence the Amplex Red/HRP/H_2O_2 fluorescence readout under conditions relevant to high-voltage electric pulse treatment. The results show that the assay response is highly context-dependent.

Phosphate-buffered saline, HB1 buffer, complete DMEM, and distilled water were treated with electrical pulses and the formation of hydrogen peroxide as a result of this treatment was evaluated by using Amplex Red, which is a fluorogenic probe for H_2O_2 detection [8,16]. It turned out that the fluorescence of resorufin, which is the product of the reaction of Amplex Red with H_2O_2 catalyzed by the horseradish peroxidase (HRP), depends not only on the parameters of electric treatment, such as, pulse amplitude, duration, and number. The intensity of fluorescence differed markedly between PBS, HB1 buffer, complete DMEM, and distilled water (Figure 1).

Main factors affecting the fluorescence of Amplex Red/HRP/H_2O_2 system in electric pulse treated media, such as, the electical conductivity of the medium, its composition and pH and as well as various metal ions, which can be released from the electrodes during high-voltage pulses, have been studied. Because the intensity of electrochemical reactions during electric pulse treatment depends strongly on electric current density, which is determined by the electrical conductivity of the medium, it was expected that the intensity of the hydrogen peroxide formation would depend on the specific conductance of each medium. To ascertain whether this assumption is correct, the electrical conductivities of the tested media were determined and compared with their corresponding pulse-induced fluorescence responses (Figure 2).

The results obtained provide some explanation for the medium-dependent pulse responses albeit incomplete one. Electrical conductivities of the media used in this study followed the order PBS > HB1 buffer > complete DMEM > distilled water (Figure 2a), which broadly paralleled the pulse-induced fluorescence trend (Figure 2b). This agrees with the expectation that electrochemical reactions at the electrode–solution interface depend on current density and therefore on medium conductivity. However, conductivity did not fully explain the fluorescence response. HB1 had conductivity close to PBS but produced substantially lower fluorescence, while complete DMEM also showed a response that could not be predicted from conductivity alone. Therefore, pulse-induced Amplex Red fluorescence reflects at least two overlapping processes: electrochemical oxidant generation during pulse exposure and medium-dependent performance of the Amplex Red/HRP/H_2O_2 system. Buffer composition, pH stability, ionic strength, peroxide-scavenging components, amino

acids, and serum-derived constituents in complete DMEM may all contribute to the final fluorescence output.

Even when identical nominal H_2O_2 concentrations were used, fluorescence intensity differed markedly between PBS, HB1 buffer, complete DMEM, and distilled water, which were not treated with electric pulses (Figure 3). In addition, electric pulse-treated samples showed strong dependence on medium conductivity (Figure 2) and pulse conditions (Figure 1), while electrode-relevant metal ions directly suppressed the apparent fluorescence signal (Figures 5–8). These findings demonstrate that Amplex Red fluorescence in pulse-treated media cannot be interpreted as a direct and interference-free measure of H_2O_2 without appropriate controls.

The medium-comparison experiments demonstrated a pronounced matrix dependence of the Amplex Red/HRP/H_2O_2 fluorescence response, with PBS producing the highest signal and distilled water the lowest. This finding is important because Amplex Red-based H_2O_2 estimation usually relies on comparison with a calibration curve. If calibration standards and experimental samples are prepared in different media, the calculated H_2O_2 concentration may be substantially biased. The observed medium dependence suggests that the chemical matrix affects HRP-catalyzed Amplex Red oxidation, resorufin fluorescence, peroxide availability, or a combination of these factors. This interpretation is consistent with previous reports showing that quantitative use of the Amplex Red assay depends on pH, H_2O_2 concentration range, and reaction conditions [19] and that reducing compounds such as NADH and reduced glutathione can interfere with the signal [23]. Komlódi et al. also showed that Amplex UltraRed-based H_2O_2 flux measurements can be affected by medium-specific background fluorescence and H_2O_2-independent artifacts, reinforcing the need for medium-specific controls [15].

The different fluorescence responses observed in PBS, HB1 buffer, complete DMEM, and distilled water can be explained by the different chemical environments provided by these media. The Amplex Red assay depends on HRP-catalyzed oxidation of Amplex Red by H_2O_2 to form fluorescent resorufin; therefore, any factor that affects HRP activity, H_2O_2 availability, Amplex Red oxidation, or resorufin fluorescence can alter the final signal [16,19,20,23]. PBS is a relatively simple, well-buffered salt solution and therefore provides favorable and reproducible conditions for the HRP/Amplex Red reaction. HB1 buffer also provides buffering capacity and physiological salts, but its different ionic composition and the presence of glucose may alter the enzyme microenvironment, peroxide stability, or fluorescence yield compared with PBS. Complete DMEM is substantially more chemically complex because it contains inorganic salts, amino acids, vitamins, glucose, phenol red, serum-derived proteins and other components. These constituents may scavenge H_2O_2, act as reducing or redox-active species, interact with HRP, contribute to background absorbance/fluorescence, or partially suppress resorufin fluorescence [8,23,24]. Future studies using resorufin-spiking or post-reaction dilution controls will be needed to distinguish whether the lower signal in complete DMEM mainly reflects reduced HRP-mediated Amplex Red oxidation, altered H_2O_2 availability, optical/background effects, or direct effects on resorufin fluorescence. Distilled water, in contrast, has very low ionic strength and essentially no buffering capacity, which may reduce HRP reaction efficiency and make resorufin fluorescence more sensitive to changes in pH.

Thus, the observed order of fluorescence intensity, PBS > HB1 > complete DMEM > distilled water, should not be interpreted as reflecting differences in the nominal H_2O_2 concentration alone. Instead, it indicates that the Amplex Red/HRP/H_2O_2 readout is strongly matrix-dependent. This is particularly important in electric pulse experiments, where electrochemical reactions at the electrode surface may further change local pH [25], generate redox-active species [8], and release metal ions [4–7,9–14]. Such ions may consume

H_2O_2 through Fenton-type reactions or interfere directly with Amplex Red/resorufin fluorescence [15,26]. Therefore, medium-matched calibration curves and spike-recovery controls are necessary when Amplex Red is used for quantitative H_2O_2 assessment in electroporation-related media.

The pulse-parameter experiment provides a key methodological warning. Under short-pulse conditions, fluorescence increased with voltage, which is consistent with the expectation that stronger electrical input increases electrochemical activity. However, under the longer pulse condition, the fluorescence signal no longer increased monotonically; a stronger pulse condition produced a lower signal than a weaker pulse condition. This signal inversion indicates that stronger electrical treatment does not necessarily result in higher measured Amplex Red fluorescence. Possible contributors include electrode-derived products, local pH shifts near the electrode surfaces, peroxide consumption, HRP inhibition, resorufin quenching, or direct redox interactions with Amplex Red. Additional pulse-related effects, such as gas bubble formation, local heating, electrolysis-driven acidification or alkalinization, may also contribute [6,7]. Degradation or redox conversion of Amplex Red/resorufin at the electrode interface may additionally affect the fluorescence response [15,19,23]. However, bulk pH was not measured immediately after each pulse condition, and local pH changes near the electrodes cannot be excluded. Similar concerns have been raised for Amplex-type assays, where fluorescence may be influenced by background oxidation or interfering redox reactions rather than H_2O_2 alone [15,19,23]. Therefore, in pulse-treated systems, a lower fluorescence signal should not automatically be interpreted as lower H_2O_2 formation.

The detection of nickel and chromium ions in pulse-treated 0.9% NaCl confirms that stainless-steel electrodes are not chemically inert under the tested pulse conditions. Both Ni and Cr concentrations increased with electric field strength, showing that electrode-derived contaminants can accumulate in the treated medium. This agrees with earlier studies showing that stainless-steel electrodes can release metal ions during electroporation or pulsed electric field exposure [5,9–11,27]. The recent study by Maček Lebar et al. provides particularly relevant support, showing that electrode dissolution during electroporation releases metal byproducts into the medium and that stainless-steel electrodes, especially under longer pulse protocols, can increase iron, chromium, and nickel concentrations [26]. The present study extends this issue to analytical fluorescence measurements by showing that electrode-relevant metal ions can directly suppress the Amplex Red/HRP/H_2O_2 fluorescence signal. Thus, corrosion products may lead to underestimation or distortion of apparent H_2O_2 formation in pulse-treated media.

Among the tested ions, Fe^{2+} produced the strongest fluorescence suppression, particularly at a low H_2O_2 concentration. At 0.4 µM H_2O_2, Fe^{2+} reduced fluorescence by up to 92%, followed by Fe^{3+}, Cr^{6+}, and Al^{3+} (Figure 7). This result is chemically plausible because Fe^{2+} can react with H_2O_2 through Fenton reactions, consuming peroxide and generating hydroxyl radicals [24,28]:

$$Fe^{2+} + H_2O_2 \rightarrow Fe^{3+} + {}^{\bullet}HO + H_2O \quad (1)$$

$$Fe^{3+} + H_2O_2 \rightarrow Fe^{2+} + O_2 + H^+ \quad (2)$$

$$H_2O_2 + {}^{\bullet}OH \rightarrow HO_2{}^{\bullet} + H_2O \quad (3)$$

In the context of the Amplex Red assay, H_2O_2 consumption would reduce substrate availability for HRP-mediated resorufin formation, while secondary radical products may further affect Amplex Red or resorufin. Although the present experiments do not distinguish these mechanisms directly, the stronger Fe^{2+} effect at 0.4 µM H_2O_2 than at 10 µM H_2O_2 suggests that competition for or depletion of available H_2O_2 through Fenton-

type reactions is likely an important contributor, while direct redox effects on Amplex Red/resorufin or fluorescence quenching cannot be excluded. Fe^{3+} also reduced fluorescence, although less strongly than Fe^{2+}, suggesting that iron-mediated interference is not restricted to the reduced form and may involve redox cycling, complexation, or indirect effects on assay components. The suppressive effects of Al^{3+} and Cr^{6+} were weaker but still evident, showing that non-iron electrode-relevant ions can also distort the assay. Importantly, the relative suppressive effects were lower at 10 μM H_2O_2 than at 0.4 μM H_2O_2, indicating that low-peroxide measurements are especially vulnerable to interference.

The pH-dependent fluorescence measurements further show that the Amplex Red readout is sensitive to the pH and buffer compositions (Figure 8). This agrees with Towne et al., who reported that HRP-catalyzed oxidation of dihydroxyphenoxazine derivatives depends strongly on pH and H_2O_2 concentration [19]. This sensitivity is particularly relevant to electric pulse experiments because water electrolysis at electrode surfaces can generate H^+ near the anode and OH^- near the cathode [7,25]. In unbuffered or weakly buffered media, such as distilled water, these local pH shifts may substantially alter the assay environment. Even in buffered media, the local pH near the electrode surface may deviate from the bulk pH during pulse exposure [25]. Therefore, pH and buffer capacity provide an additional explanation for why conductivity alone does not predict the fluorescence response across media.

In addition, the appearance of the ions of iron and aluminum in the medium changes its pH. This is because these ions behave as a Lewis acid and undergo spontaneous hydrolysis reactions, e.g., [12]:

$$Fe^{2+} + nH_2O \leftrightarrow Fe(OH)_n{}^{3-n+} + nH^+. \quad (4)$$

Because the fluorescence of Amplex Red/HRP/H_2O_2 system strongly depends on the medium pH (the lower the pH the weaker fluorescence is), appearance of iron or aluminum ions in the medium leads to the reduction of the fluorescence not only because H_2O_2 can be consumed as a result of Fenton reactions but because of decrease in the medium pH caused by these ions.

The present findings do not mean that Amplex Red is unsuitable for electroporation studies. Amplex Red and related ADPH-based systems remain useful for ROS-responsive fluorescence detection, as illustrated by their continued use in biological imaging and controlled analytical systems [17,18]. However, the present data show that in pulse-treated media, Amplex Red fluorescence cannot be treated as an interference-free standalone measure of H_2O_2. For reliable use of the assay in electroporation-related experiments, several controls are necessary. First, calibration curves should be prepared in the same medium as the experimental samples. Second, spike-recovery experiments should be performed to determine whether known H_2O_2 additions are recovered accurately after pulse exposure. Third, metal-ion controls should be included when stainless-steel or other dissolvable electrodes are used. Fourth, pH and conductivity should be monitored or controlled, particularly in weakly buffered media. Fifth, where quantitative hydrogen peroxide determination is required, Amplex Red fluorescence should ideally be supported by complementary approaches, such as catalase controls, electrochemical H_2O_2 detection [29], or other orthogonal ROS-detection methods [30]. For practical H_2O_2 measurements in electroporated cell suspensions prepared in complete DMEM using stainless-steel electrodes, we consider the minimum control set to include medium-matched H_2O_2 calibration, non-pulsed cell-containing controls, pulse-treated medium-only controls, H_2O_2 spike-recovery controls under the same medium/electrode conditions, and catalase-treated controls to confirm H_2O_2-dependent signal contribution.

Several limitations should be acknowledged. The present experiments do not distinguish between direct quenching of resorufin fluorescence, Fenton-mediated H_2O_2 con-

sumption, HRP inhibition, and degradation of Amplex Red or resorufin by secondary radicals. Mechanistic experiments using pre-formed resorufin would help clarify whether metal ions suppress fluorescence by quenching the fluorescent product directly or by interfering with its formation. Because chromium release was detected from stainless-steel electrodes [9], Cr^{6+} was included in the present interference experiment as a soluble and chemically well-defined chromium-containing redox-active model species to assess whether chromium-related compounds may interfere with the Amplex Red/HRP/H_2O_2 readout. Chromium speciation in pulse-treated media may vary depending on electrode material, pulse parameters, pH, oxygen availability, and medium composition [9–11]. Because Cr^{3+} differs from Cr^{6+} in solubility, hydrolysis, complexation, and precipitation behavior, especially in phosphate- or protein-containing media [31], its effect on the assay may differ and would require separate controlled experiments.

In addition, although Ni and Cr release from stainless-steel electrodes was detected, Ni^{2+} was not directly tested in the Amplex Red assay. Furthermore, the present study evaluated metal ions individually and did not examine mixed-ion systems, although pulse-treated media may contain several electrode-derived ions simultaneously, and these mixtures may produce additive, antagonistic, or synergistic effects on the fluorescence readout. Therefore, future studies should evaluate mixed-ion combinations that more closely reproduce the chemical composition of pulse-treated electroporation media. The tested metal-ion concentrations, particularly for iron, also exceed the bulk concentrations typically measured after pulse exposure [4,5,9,12], although localized concentrations near the electrode surface may be higher. Finally, the pH experiments were performed in buffer systems rather than during real-time pulse exposure, so the combined effects of pulse-induced pH shifts, metal-ion release, and Amplex Red chemistry remain to be investigated.

In summary, the Amplex Red/HRP/H_2O_2 fluorescence readout in electroporation-relevant systems is shaped by multiple interacting factors, including medium composition, conductivity, pulse parameters, pH/buffer conditions, and electrode-derived metal ions. The practical implication is that Amplex Red should not be used as a standalone, interference-free H_2O_2 probe in pulse-treated media. Instead, the fluorescence signal should be interpreted as an assay-dependent readout that requires appropriate medium-specific, pulse-condition, pH, and metal-ion controls.

5. Conclusions

This study demonstrates that the Amplex Red/HRP/H_2O_2 fluorescence readout is strongly influenced by the chemical environment under conditions relevant to high-voltage electric pulse treatment. Medium composition, conductivity, pulse parameters, pH, and electrode-relevant metal ions all affected the measured fluorescence signal. Notably, the fluorescence response is not always proportional to the applied pulse conditions, indicating that stronger electrical treatment does not necessarily result in higher measured Amplex Red fluorescence. Fe^{2+} and Fe^{3+} produced the strongest fluorescence suppression, especially at low H_2O_2 concentration, while Al^{3+} and Cr^{6+} showed weaker but still detectable effects. These findings indicate that Amplex Red fluorescence in pulse-treated systems should not be interpreted as an interference-free quantitative measure of H_2O_2. For reliable application in electroporation-related experiments, the assay should be supported by medium-matched calibration, spike-recovery experiments, metal-ion controls, and, where necessary, complementary validation approaches.

Author Contributions: Conceptualization, G.S.; methodology, R.R., L.Z.-H. and G.S.; validation, R.R., R.S. and G.S.; formal analysis, L.Z.-H.; investigation, L.Z.-H., R.R., V.S.D., K.R. and R.S.; resources, R.S., Y.H. and G.S.; data curation, L.Z.-H., V.S.D. and K.R.; writing—original draft preparation, L.Z.-H. and Y.H.; writing—review and editing, R.R., Y.H. and G.S.; visualization, L.Z.-H., V.S.D., K.R. and

Y.H.; supervision, G.S.; project administration, G.S. and R.S.; funding acquisition, R.S. and G.S. All authors have read and agreed to the published version of the manuscript.

Funding: This research was supported by the Research Council of Lithuania (grant number S-MIP-20-29) to G.S. L.Z.-H. was supported by a Ph.D. grant from the Research Council of Lithuania (LMTLT), grant number NKPDOKT-15131 (to R.S.).

Institutional Review Board Statement: Not applicable.

Informed Consent Statement: Not applicable.

Data Availability Statement: The raw data supporting the conclusions of this article will be made available by the authors upon request.

Conflicts of Interest: The authors declare no conflicts of interest.

References

1. Neumann, E.; Schaefer-Ridder, M.; Wang, Y.; Hofschneider, P.H. Gene transfer into mouse lyoma cells by electroporation in high electric fields. *EMBO J.* **1982**, *1*, 841–845. [CrossRef] [PubMed]
2. Gehl, J. Electroporation: Theory and methods, perspectives for drug delivery, gene therapy and research. *Acta Physiol. Scand.* **2003**, *177*, 437–447. [CrossRef] [PubMed]
3. Milazzo, G. *Electrochemistry: Theoretical Principles and Practical Applications*; Elsevier: Amsterdam, The Netherlands, 1963.
4. Kotnik, T.; Miklavčič, D.; Mir, L.M. Cell membrane electropermeabilization by symmetrical bipolar rectangular pulses. Part II. Reduced electrolytic contamination. *Bioelectrochemistry* **2001**, *54*, 91–95. [CrossRef] [PubMed]
5. Tomov, T.; Tsoneva, I. Are the stainless steel electrodes inert? *Bioelectrochemistry* **2000**, *51*, 207–209. [CrossRef] [PubMed]
6. Saulis, G.; Lape, R.; Pranevičiūtė, R.; Mickevičius, D. Changes of the solution pH due to exposure by high-voltage electric pulses. *Bioelectrochemistry* **2005**, *67*, 101–108. [CrossRef] [PubMed]
7. Saulis, G.; Rodaitė-Riševičienė, R.; Dainauskaitė, V.S.; Saulė, R. Electrochemical processes occurring during high-voltage electric pulses and their importance for the technology of food processing by pulsed electric fields. In *Advances in Food Biotechnology*; Ravishankar Rai, V., Ed.; John Wiley & Sons: West Sussex, UK, 2016; pp. 575–591.
8. Pakhomova, O.N.; Khorokhorina, V.A.; Bowman, A.M.; Rodaitė-Riševičienė, R.; Saulis, G.; Xiao, S.; Pakhomov, A.G. Oxidative effects of nanosecond pulsed electric field exposure in cells and cell-free media. *Arch. Biochem. Biophys.* **2012**, *527*, 55–64. [CrossRef] [PubMed]
9. Roodenburg, B.; Morren, J.; Berg, H.E.I.; de Haan, S.W.H. Metal release in a stainless steel pulsed electric field system. Part I. Effect of different pulse shapes; theory and experimental method. *Innov. Food Sci. Emerg. Technol.* **2005**, *6*, 327–336. [CrossRef]
10. Pataro, G.; Falcone, M.; Donsì, G.; Ferrari, G. Metal release from stainless steel electrodes of a PEF treatment chamber: Effects of electrical parameters and food composition. *Innov. Food Sci. Emerg. Technol.* **2014**, *21*, 58–65. [CrossRef]
11. Ruzgys, P.; Novickij, V.; Novickij, J.; Šatkauskas, S. Influence of the electrode material on ROS generation and electroporation efficiency in low and high frequency nanosecond pulse range. *Bioelectrochemistry* **2019**, *127*, 87–93. [CrossRef] [PubMed]
12. Saulis, G.; Rodaitė-Riševičienė, R.; Saulė, R. Cytotoxicity of a cell culture medium treated with a high-voltage pulse using stainless steel electrodes and the role of iron ions. *Membranes* **2022**, *12*, 184. [CrossRef] [PubMed]
13. Stapulionis, R. Electric pulse-induced precipitation of biological macromolecules in electroporation. *Bioelectrochem. Bioenerg.* **1999**, *48*, 249–254. [CrossRef] [PubMed]
14. Loomis-Husselbee, J.W.; Cullen, P.J.; Irvine, R.F.; Dawson, A.P. Electroporation can cause artefacts due to solubilization of cations from the electrode plates. *Biochem. J.* **1991**, *277*, 883–885. [CrossRef] [PubMed]
15. Komlódi, T.; Sobotka, O.; Gnaiger, E. Facts and artefacts on the oxygen dependence of hydrogen peroxide flux using Amplex UltraRed. *Bioenerg. Commun.* **2021**, *2021*, 4.
16. Zhou, M.; Diwu, Z.; Panchuk-Voloshina, N.; Haugland, R.P. A stable nonfluorescent derivative of resorufin for the fluorometric determination of trace hydrogen peroxide. *Anal. Biochem.* **1997**, *253*, 162–168. [CrossRef] [PubMed]
17. Metro, J.; Reitemeier, J.; Bohn, P.W. Enzyme dynamics in attoliter-volume electrochemical zero-mode waveguides with on-demand in situ hydrogen peroxide delivery and consumption. *Appl. Spectrosc.* **2025**, *79*, 1313–1324. [CrossRef] [PubMed]
18. Sun, K.; Xu, R.; Xue, B.; Liu, P.; Bai, J.; Tian, Y.; Li, X.; Tang, Q. ROS-responsive ADPH nanoparticles for image-guided surgery. *Front. Chem.* **2023**, *11*, 1121957. [CrossRef] [PubMed]
19. Towne, V.; Will, M.; Oswald, B.; Zhao, Q. Complexities in horseradish peroxidase-catalyzed oxidation of dihydroxyphenoxazine derivatives: Appropriate ranges for pH values and hydrogen peroxide concentrations in quantitative analysis. *Anal. Biochem.* **2004**, *334*, 290–296. [CrossRef] [PubMed]
20. Lakowicz, J.R. *Principles of Fluorescence Spectroscopy*, 3rd ed.; Springer: Boston, MA, USA, 2006.

21. Vahalová, P.; Havelka, D.; Vaněčková, E.; Zakar, T.; Kolivoška, V.; Cifra, M. Biochemiluminescence sensing of protein oxidation by reactive oxygen species generated by pulsed electric field. *Sens. Actuators B Chem.* **2023**, *385*, 133676. [CrossRef]
22. Puc, M.; Corovic, S.; Flisar, K.; Petkovsek, M.; Nastran, J.; Miklavcic, D. Techniques of signal generation required for electropermeabilization. Survey of electropermeabilization devices. *Bioelectrochemistry* **2004**, *64*, 113–124. [CrossRef] [PubMed]
23. Votyakova, T.V.; Reynolds, I.J. Detection of hydrogen peroxide with Amplex Red: Interference by NADH and reduced glutathione auto-oxidation. *Arch. Biochem. Biophys.* **2004**, *431*, 138–144. [CrossRef] [PubMed]
24. Stohs, S.J.; Bagchi, D. Oxidative mechanisms in the toxicity of metal ions. *Free Radic. Biol. Med.* **1995**, *18*, 321–336. [CrossRef] [PubMed]
25. Meneses, N.; Jaeger, H.; Knorr, D. pH-changes during pulsed electric field treatments. Numerical simulation and *in situ* impact on polyphenoloxidase inactivation. *Innov. Food Sc. Emerg. Technol.* **2011**, *12*, 499–504. [CrossRef]
26. Maček Lebar, A.; Potočnik, T.; Ščančar, J.; Marković, S.; Polajžer, T. Bystander effect of metal byproducts released from electroporated cells after electroporation in vitro. *Bioelectrochemistry* **2025**, *164*, 108940. [CrossRef]
27. Rodaitė-Riševičienė, R.; Saulė, R.; Snitka, V.; Saulis, G. Release of iron ions from the stainless steel anode occurring during high-voltage pulses and its consequences for cell electroporation technology. *IEEE Trans. Plasma Sci.* **2014**, *42*, 249–254.
28. Winterbourn, C.C. Toxicity of iron and hydrogen peroxide: The Fenton reaction. *Toxicol. Lett.* **1995**, *82–83*, 969–974. [CrossRef] [PubMed]
29. Liu, J.; Li, M.; Liu, W.; Hao, Z.; Zhang, F.; Pang, H.; Zhang, R.; Zhang, L. Advances in non-enzymatic electrochemical materials for H_2O_2 sensing. *J. Electroanal. Chem.* **2024**, *954*, 118060. [CrossRef]
30. Murphy, M.P.; Bayir, H.; Belousov, V.; Chang, C.J.; Davies, K.J.A.; Davies, M.J.; Dick, T.P.; Finkel, T.; Forman, H.J.; Janssen-Heininger, Y.; et al. Guidelines for measuring reactive oxygen species and oxidative damage in cells and in vivo. *Nat. Metab.* **2022**, *4*, 651–662. [CrossRef] [PubMed]
31. Rai, D.; Sass, B.M.; Moore, D.A. Chromium(III) hydrolysis constants and solubility of chromium(III) hydroxide. *Inorg. Chem.* **1978**, *26*, 345–349.

Disclaimer/Publisher's Note: The statements, opinions and data contained in all publications are solely those of the individual author(s) and contributor(s) and not of MDPI and/or the editor(s). MDPI and/or the editor(s) disclaim responsibility for any injury to people or property resulting from any ideas, methods, instructions or products referred to in the content.